JOURNAL OF VIROLOGY, Aug. 1988, p. 2736–2744
0022-538X/88/082736-09$02.00/0

Vol. 62, No. 8

Generation and Characterization of a Temperature-Sensitive Mutation in the NS-1 Gene of the Autonomous Parvovirus Minute Virus of Mice

GREGORY E. TULLIS, LAURA LABIENIEC-PINTEL, KAREN E. CLEMENS, AND DAVID PINTEL*
Department of Microbiology, School of Medicine, University of Missouri–Columbia, Columbia, Missouri 65212

Received 26 February 1988/Accepted 18 April 1988

In-phase single-codon insertion mutations were constructed in the open reading frames of the NS-1 and NS-2 genes of the autonomous parvovirus minute virus of mice. A viral mutant containing an isoleucine insertion exclusively within NS-1 between residues 229 and 230 was isolated that produced approximately 3 orders of magnitude fewer plaques at 39°C than at 32°C. Preliminary characterization of the mutant demonstrated that the NS-1 gene product is independently required for both genome amplification and the regulation of the temporal expression between the two viral transcription units during lytic infection.

The autonomous parvovirus minute virus of mice (MVM) contains a linear, single-stranded DNA genome about 5.1 kilobases (kb) in length with nonidentical hairpin structures found at palindromes present at both ends of the genomic DNA (6, 17, 50). The MVM(p) genome, like that of all other known parvoviruses, is organized into two major coding regions (9, 17). The left half of the MVM genome encodes two nonstructural proteins, NS-1 (83 kilodaltons) and NS-2 (25 kilodaltons) (3, 16), and the right half of the genome codes for the capsid proteins VP1 and VP2 (3, 25).

These coding regions are expressed from two overlapping transcription units which produce three major cytoplasmic mRNA species (39). Transcripts R1 (4.8 kb) and R2 (3.3 kb) are initiated at a promoter near the left-hand end of the genome at approximately nucleotide (nt) 201, and the R3 (3.0-kb) transcript is initiated at approximately nt 2005 (3, 8, 39). NS-1 and NS-2 are translated from the R1 and R2 transcripts (15, 16), respectively, and the viral capsid proteins VP1 and VP2 are translated from the viral 3.0-kb R3 messages (3, 25). The two transcription units of MVM are expressed in a temporal order; the appearance of the viral R1 and R2 messages precedes the R3 messages (13). All viral mRNAs are polyadenylated near the right-hand end of the genome at approximately nt 4908 (12) and share three possible splicing patterns between nts 2280 and 2399 (3, 6, 23, 35). The R2 message is, in addition, spliced between nts 516 and 1990 (23).

NS-1 is translated from R1 in open reading frame (ORF) 3, beginning at nt 261 and terminating at nt 2278, prior to the R1 small intron (Fig. 1) (16). NS-2 also initiates at nt 261. The amino-terminus exon of NS-2 is translated from R2 in ORF 3 and is identical to NS-1 for 84 amino acids (16). Exon 2 of NS-2 is translated in ORF 2 (16). Alternative splicing of the R2 message between nts 2280 and 2399 may generate three forms of NS-2 with different carboxyl termini (3, 6, 23, 35). Proteins similar to the nonstructural proteins of MVM are encoded by numerous other autonomous parvoviruses (17). An analogous but somewhat different set of nonstructural proteins is synthesized by the parvoviruses bovine parvovirus (28, 29), B19 (14, 36), and the dependovirus adeno-associated virus type 2 (33).

The functions of the nonstructural proteins during parvovirus infection have not been fully determined; however, they are clearly multiple. The nonstructural proteins of adeno-associated virus type 2 have been shown to be required for virus replication (21, 43, 51). The role(s) of the nonstructural proteins of MVM in viral DNA replication is uncertain. However, the NS-1 protein of MVM is required for infectivity of plasmid clones of MVM DNA (M. J. Merchlinsky, Ph.D. thesis, Yale University, New Haven, Conn., 1984). Whether this latter requirement is at the level of initial excision from plasmid sequences or at subsequent steps in replication has not been definitively determined. The nonstructural proteins of both autonomous and nonautonomous parvoviruses have been shown to stimulate the expression of reporter gene products driven by capsid gene promoters in transient cotransfection assays (27, 40, 41, 52). The adeno-associated virus type 2 nonstructural proteins have, under certain conditions, been shown also to regulate these promoters negatively (27, 52) and to influence the translation of capsid gene mRNA as well (53). Parvovirus nonstructural proteins also inhibit expression from numerous heterologous viral promoters transfected on plasmids (26). MVM NS-1 has been shown to be covalently attached to the 5′ end of both MVM genomic single-stranded and double-stranded replicative form (RF) DNA (18). It has also been suggested to possess the topoisomerase I type nicking activity that current models of MVM DNA replication invoke (2, 5, 49).

Genetic and functional analysis of the nonstructural proteins of the autonomous parvoviruses during lytic infection has proved difficult. Analysis of lethal mutations in the infectious plasmid clone of MVM has been hindered by the very low infectivity of cloned DNA. Cell lines which constitutively express the nonstructural proteins and which might complement and propagate such lethal mutants are not easily constructed owing to the apparent toxicity of these proteins and their inhibitory effect on the expression of cotransfected selectable markers (26, 41; R. V. Schoborg and D. Pintel, unpublished observation).

To overcome these barriers to studying the function of the nonstructural proteins, we attempted to generate temperature-sensitive mutants in NS-1 and NS-2 of MVM(p). We chose to utilize the single-amino-acid insertion technique described by Bernstein et al. (10). Use of a similar technique in procaryotic systems has been reported to yield a high

* Corresponding author.

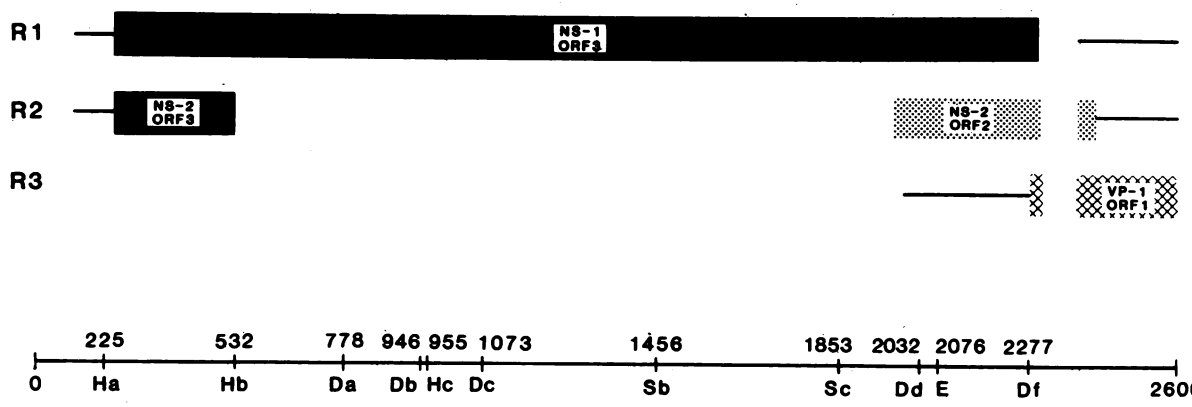

FIG. 1. Map displaying putative codon insertion mutations in relation to the NS-1-NS-2 coding region. The upper part of the figure shows the exons of three major viral mRNAs, R1, R2, and R3, in the left 2,600 nucleotides of MVM. ORFs encoding NS-1 (solid box), NS-2 (solid and stippled boxes), and VP1 (hatched boxes) are indicated. The bottom line represents the MVM genome from nts 0 to 2600 and shows the location of the codon insertion mutations discussed in this report. The first letter of the mutation designation refers to the restriction enzyme with which it was made (H, *Hin*fI; D, *Dde*I; S, *Sau*96I; E, *Eco*O109I), and the second letter designates the restriction enzyme site, starting from the left-hand end.

percentage of conditionally lethal mutations (7). In this paper, we report the generation of a mutation in the MVM(p) NS-1 gene which renders the virus approximately 1,000-fold temperature sensitive in plaque-forming ability at 39°C. Characterization of this mutant demonstrated directly that MVM(p) NS-1 is required for both viral genome amplification and the regulation of the temporal expression of transcripts from the two viral transcription units during lytic infection.

MATERIALS AND METHODS

Cells and viruses. Murine A92L (31) and A9ouab^{r}11 (47) and human NB324K (45) cells were passaged and maintained and MVM(p) was propagated, harvested, and assayed as previously described (47, 48). Cells were synchronized in G1 by isoleucine deprivation for 46 to 48 h (30) (parasynchronous) or at the G1-S border by a combination of isoleucine deprivation for 46 to 48 h followed by treatment with the alpha-DNA polymerase inhibitor aphidicolin for 20 h (13, 17, 20, 38) (highly synchronized). For viral infection of highly synchronized cells, virions were added 10 h before release of the cells from aphidicolin. Plaque isolation and propagation of virions were as described previously (47, 48), except that parasynchronized cells were used for the early passage of plaques. Growth curves were determined by infecting parallel cultures of 10^5 parasynchronized A9ouab^{r}11 cells in duplicate 60-mm^2 dishes at 32 or 39°C with either mutant or wild-type virus at a multiplicity of infection of 1. For the growth curve, virions were added at the time of release of the cells into complete medium. DNA transfections as $CaPO_4$ precipitates were as previously described (25).

Mutant construction. Restriction enzymes and DNA and RNA polymerases were purchased from either New England BioLabs, Inc. (Beverly, Mass.) or Promega Biotec (Madison, Wis.). Amino acid insertion mutants were constructed as described by Bernstein et al. (10) with minor modifications. A *Bam*HI-to-*Stu*I fragment (1 to 2378) from the infectious clone of MVM was cloned into a pBR322 derivative. The plasmid was linearized with *Dde*I, *Hin*fI, or *Sau*96I in the presence of 10 to 100 μg of ethidium bromide per ml (empirically determined for each enzyme and each DNA preparation) (37). Linear DNA was isolated, filled in with the large fragment of DNA polymerase I, religated, and used to transform *Escherichia coli* HB101. Transformants were screened for the loss of a restriction site in the MVM NS-1 or NS-2 gene. Potential in-phase codon insertion mutations, Da, Db, Df, Ha, and Sc, were inserted into the infectious clone of MVM by using a *Bam*HI-to-*Nar*I (0 to 2290) fragment, and mutations Dc, Dd, Hb, Hc, and Sb were reconstructed with *Eco*RV-to-*Xho*I (384 to 2071) fragments. The *Sau*96I-*Eco*O109I site at 2076 was resistant to cleavage owing to overlapping *dcm* methylation. Molecules linearized at this site with *Eco*O109I were obtained in cloned MVM grown in the methylase-negative strain GM119 (1). To restore infectivity in this clone, we rebuilt the right-hand end from the *Xba*I site (4340) from the infectious clone of MVM. Potentially infectious clones were propagated in *E. coli* JC8111 (11).

Analysis of viral DNA and RNA. Hirt extraction (22) of viral DNA from infected cells and subsequent Southern analysis were as previously described (46). Probes for Southern analysis were prepared by nick translation (32). RNA was extracted from cells lysed in guanidine hydrochloride and was purified by centrifugation through a CsCl cushion as described previously (32). Quantitative RNase protection assays, done in probe excess, and subsequent gel analyses were done as described previously (13). DNA sequencing was by the dideoxy-chain termination method (42) with the Sequenase enzyme (U.S. Biochemicals, Cleveland, Ohio).

RESULTS

Construction and initial characterization of single-amino-acid insertion mutants. Single-codon insertion mutations were introduced into the NS-1-NS-2 coding region of MVM by digestion with restriction enzymes, which produced three nucleotide overhangs, and filling in these ends with the large fragment of DNA polymerase I (10). To minimize the number of restriction sites for the enzymes of interest and to direct the mutations to the NS-1-NS-2 coding region, we cloned the left half of the MVM genome (Fig. 1) into a small pBR322 derivative composed primarily of the ampicillin resistance gene and the origin of replication. The plasmids were partially digested with *Dde*I, *Hin*fI, or *Sau*96I in the presence of ethidium bromide as described in Materials and Methods to maximize the yield of singly cut linear DNA. This DNA was then isolated, filled in, religated, and used to

TABLE 1. Compilation of putative codon insertion mutations in the NS-1-NS-2 coding region

Mutation[a]	Position (nt)	Predicted insertion		Phenotype[b]
		NS-1	NS-2	
Ha	225			WT
Hb	532	Tyr		TS
Da	778	Ile		NV
Db[c]	946	Ile		TS
Hc	955	Tyr		NV
Dc	1073	Asn		NV
Sb	1456	Arg		NV
Sc	1853	Pro		NV
Dd	2032	Ile	His	WT
E	2076	Asp	Arg	TS
Df	2277		Ile	NV

[a] See legend to Fig. 1 for explanation of mutation designations.
[b] Phenotype when inserted into the infectious clone of MVM. WT, Wild type; TS, temperature sensitive; NV, nonviable.
[c] Two independently isolated mutations at the *Dde*I site at 946 (Db-1 and Db-2) were characterized further.

transform *E. coli* HB101. Transformants were screened for the loss of a restriction site in the MVM NS-1-NS-2-coding region. Full-length clones (Table 1) were obtained by substituting either an *Eco*RV (nt 384)-to-*Xho*I (nt 2071) fragment or in some cases a *Bam*HI (nt 1)-to-*Nar*I (nt 2290) fragment containing the mutations into the infectious clone of MVM and transforming *E. coli* JC8111 (11). It is necessary to propagate full-length clones of MVM in JC8111 because the right-hand end of MVM contains two nested internal repeats required for infectivity which are spontaneously deleted in most other *E. coli* strains. All mutant clones were verified by restriction analysis before transfection to ensure that both the right-hand end of the genome and the restriction sites used for cloning remained intact. Mutant clones (Table 1) were then tested for viability by DNA transfection plaque assay on mouse A9 cells at 32 and 37°C. Of the 11 mutants tested, we could not detect plaques with 6, either with or without prior excision of the MVM DNA by restriction digestion of the terminal *Bam*HI linkers initially used in constructing the infectious clone of MVM (34).

Of the five viable mutants, two appeared to be wild type by DNA transfection. One of these, designated Ha for the first *Hin*fI site (at nt 225), was altered in the leader sequence before the translational start codon for NS-1 and NS-2 (Fig. 1). The other mutation was at nt 2032 (Dd) and should produce single-amino-acid insertions in both NS-1 and NS-2. Three mutants, Hb, Db, and E, appeared to be good candidates for conditionally lethal mutants by DNA transfection. For Hb and Db, only a few small plaques were produced at 32°C and none were detected at 37°C. The inverse was true for E; small plaques were produced at 37°C and none were detected at 32°C.

Plaques from DNA transfections of Hb, Db, and E were isolated and propagated on A9 cells at the temperature at which they were originally isolated, and viral stocks were subsequently plaqued on either A9 or 324K cells at 32, 37, or 39°C (Table 2). Stocks of wild-type MVM normally produce both large and small plaques on A9 cells at all temperatures (Fig. 2). When virus from either type of plaque is propagated and reassayed, both large and small plaques are again produced, suggesting that this variability is due to the assay used rather than to a stable genetic trait (50; D. Pintel, unpublished observations). Mutant Hb stocks were marginally temperature sensitive and produced wild-type-like plaques. E stocks produced uniformly small plaques at all temperatures, with a maximum number of plaques at 37°C. Db stocks also produced small plaques at both 32°C (Fig. 2) and 39°C. They were also markedly temperature sensitive: Db stocks produced almost 1,000 times fewer plaques at 39°C than at 32°C (Table 2). When viruses from Db plaques are isolated and propagated at 32°C, they consistently produce small plaques (data not shown). The alteration predicted in Db is an isoleucine insertion between leucine 229 and serine 230 (Table 1).

In a similar way, we independently isolated another insertion mutation at the *Dde* site at 946 (termed Db-1). This mutation was substituted into the infectious clone of MVM, and viral stocks were generated which also produced approximately 1,000-fold fewer plaques at 39°C than at 32°C (Table 2). The original Db stock, designated Db-2, was chosen for further characterization.

Propagation of Db-2 at high and low temperature. Because stocks of Db-2 proved to be significantly temperature sensitive compared with wild-type stocks as measured by plaque assay, the propagation of Db-2 in culture at high and low temperature was measured. Parasynchronous subconfluent monolayers of A9 cells were infected at the time of release into the S phase at both 32 and 39°C with either Db-2 or wild-type MVM at a multiplicity of infection of 1. Virus was harvested at various times postinfection (p.i.), and titers were determined at 32°C on A9ouab^{r}11 cells (Fig. 3). All infections had reached full lysis by the final time point.

During the first 48 h of infection, Db-2 accumulation was between 10- and 100-fold less at 39°C than at 32°C, whereas wild-type accumulation was approximately equal at the two temperatures. Throughout the experiment, the total accumulation of infectious Db-2 at both 32 and 39°C was considerably less than that of wild-type virus at the comparable

TABLE 2. Plaque assays of virus stocks of wild-type MVM, two Db mutants, and an Hb and E2 mutant on A9 and NB324K cells at 32, 37, and 39°C

Mutant	PFU/ml						
	A9				NB324K		
	32°C	37°C	39°C	32°C/39°C	32°C	39°C	32°C/39°C
Wild-type MVM	1×10^8	2×10^8	1×10^8	1	3×10^9	3×10^8	10
Db-2[a]	2×10^6	ND[b]	4×10^3	5×10^2	3×10^7	1×10^3	3×10^4
Db-1[a]	4×10^5	ND	$<5 \times 10^2$	$>8 \times 10^2$	5×10^6	$<2 \times 10^2$	$>2 \times 10^4$
Hb	7×10^7	ND	4×10^6	2×10^1			
E	3×10^5	5×10^6	2×10^6				

[a] Db-1 and Db-2 are viral stocks derived from plasmid clones containing independently isolated Db mutations (see text for details).
[b] ND, Not determined.

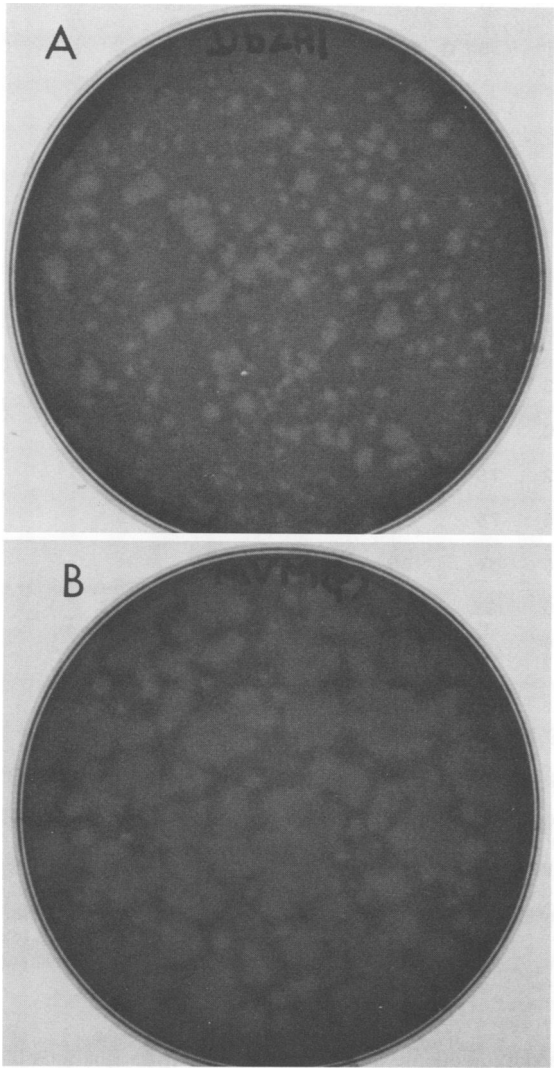

FIG. 2. Db-2 produces small plaques at 32°C. (A) Plaques of Db-2 virus at 32°C. (B) Plaques of wild-type MVM at 32°C. Plaques were assayed on A9ouab^{r}11 cells and stained after 11 days.

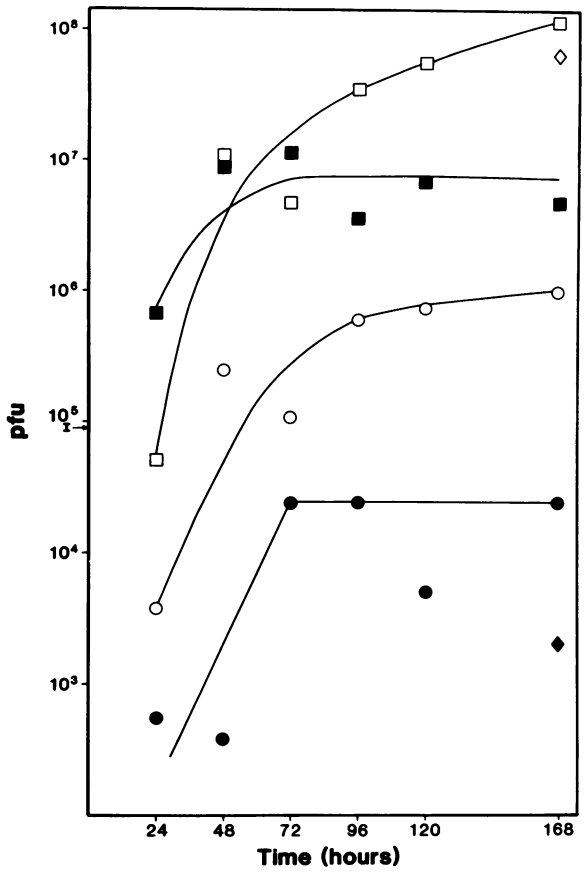

FIG. 3. Growth curves of Db-2 and wild-type MVM on A9ouab^{r}11 cells at 32 and 39°C. Growth curves were done as described in Materials and Methods. Virus titers were determined at 32°C. The ordinate is total PFU; the abscissa is time p.i. I, Input PFU for infections. Symbols: ■, wild type at 39°C; □, wild type at 32°C; ●, Db-2 at 39°C; ○, Db-2 at 32°C; ◇, wild type at 32°C, assayed at 39°C; ◆, Db-2 at 32°C, assayed at 39°C (see text for details).

temperature. The temperature sensitivity of the plaque-forming ability of Db-2 was confirmed by determining at both 32 and 39°C titers of virus taken from the final growth curve time point from both the Db-2 and wild-type infections at 32°C. This Db-2 stock also plaqued approximately 1,000-fold less at 39°C than at 32°C, compared with a less than 2-fold difference for the wild type (Fig. 3).

Marker exchange experiments. To confirm that the isoleucine insertion between residues 229 and 230 of NS-1 was solely responsible for the observed phenotype of Db-2, we conducted a series of marker exchange experiments to delimit the region responsible for the Db-2 phenotype. This was particularly important because the mutagenesis scheme involved restriction digestion in the presence of ethidium bromide. As noted earlier, however, an independently isolated insertion mutation at the *Dde*I site at nt 946 (Db-1) was similarly temperature sensitive when substituted into the infectious clone of MVM (Table 2). Because the Db-2 phenotype was evident as cloned DNA assayed by transfection (Fig. 4A), and because its defective phenotype is not overcome at even 10 μg of DNA per 60-mm^2 dish (4 × 10^5 cells) (data not shown), we proceeded to characterize a series of marker exchange constructs by DNA transfection at 32 and 37°C. All marker exchange clones were propagated in *E. coli* JC8111 and verified by restriction enzyme analysis before transfection to ensure that both the right-hand end and the restriction sites used for cloning remained intact.

In the first experiment, an *Eco*RV-*Bst*EII fragment (nts 384 to 1885) from the infectious plasmid clone of MVM was substituted into the plasmid clone of Db-2 (Fig. 4, mr1). Substitution of this wild-type fragment into Db-2 restored wild-type transfection efficiency and plaque size, indicating that outside of this region, Db-2 was similar to wild type. Therefore, the Db mutation must lie somewhere between nt 384 and nt 1885. To further narrow down this region, we performed the following additional experiments. First, the small *Eae*I fragment (nts 1 to 1030) of the infectious plasmid clone of wild-type MVM was ligated to the large *Eae*I fragment (nts 1030 to 5146) of the Db-2 plasmid clone (Fig. 4, mr2). The ligation mixture (in this case containing approximately 100 ng of uncloned 5.1-kb linear DNA per plate as estimated on an agarose gel) was applied directly to A9 cells. Plaques from this transfection appeared at a similar frequency at 32 and 37°C and were wild type in size. To confirm

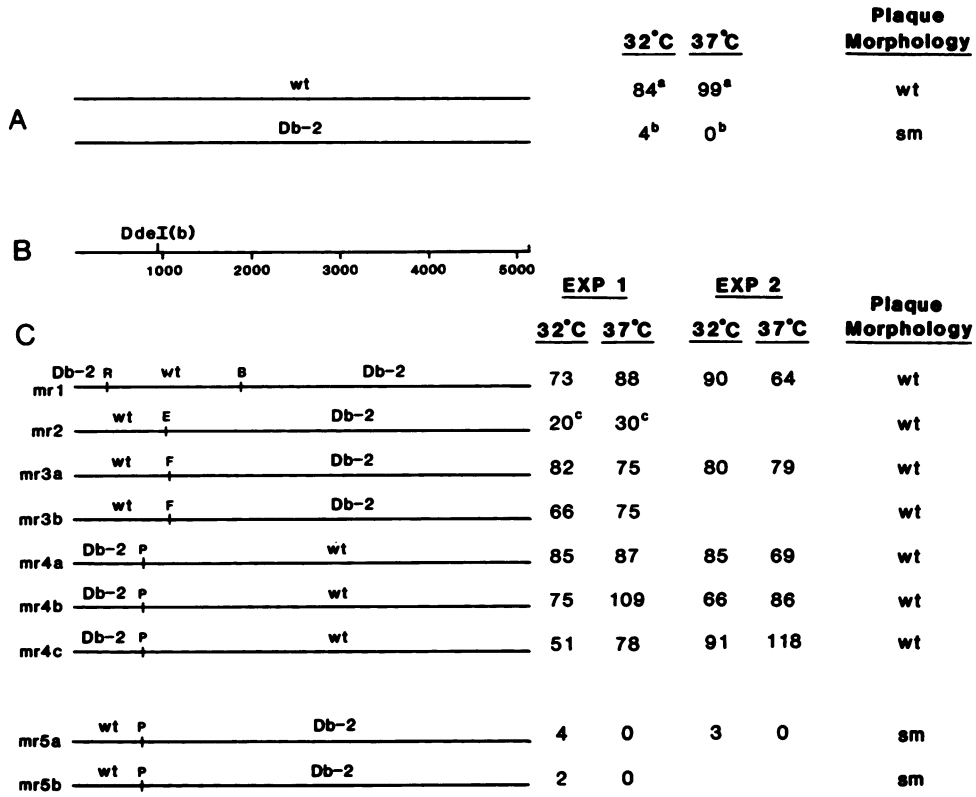

FIG. 4. Marker exchange rescue experiments confirm that that alteration responsible for the Db-2 phenotype resides between nts 763 and 1030. DNA transfection plaque assays were done at 32 and 37°C on A9ouab[r]11 cells as described in the text, using 2.5 μg of cloned DNA per 60-mm^2 dish (4×10^5 cells) (except mr2, see below). All MVM plasmids were amplified in *E. coli* JC8111 and verified by restriction digestion to ensure that both the right-hand end and the sites used for cloning remained intact. (A) Number of plaques per 60-mm^2 dish produced at 32 and 39°C by parental wild-type and Db-2 cloned DNA. (B) Location of the DdeI(b) site at nucleotide 946, the putative site of the Db-2 mutation. (C) Number of plaques per 60-mm^2 dish produced at 32 and 39°C by the various marker exchange rescue constructs (see text for details). Restriction sites: R, *Eco*RV; B, *Bst*EII; E, *Eae*I; F, *Fsp*I; P, *Pvu*II. *a*, Average of 11 experiments; *b*, average of 6 experiments; *c*, results from approximately 100 ng of uncloned full-length MVM DNA (see text for details). wt, Wild type; sm, small.

these results, we substituted the *Fsp*I fragment (0 to 1063) from cloned wild-type MVM into the Db-2 plasmid clone. Two individually isolated constructs (Fig. 4, mr3a and mr3b) were tested by DNA transfection and both performed as wild type with respect to the number of plaques obtained at 32 and 37°C and to plaque size.

The nts 1 to 763 *Pvu*II fragment from the Db-2 plasmid clone was then substituted into the wild-type MVM infectious clone. Three individually isolated constructs were tested by DNA transfection (Fig. 4, mr4a, mr4b, mr4c), and all were similar to wild type with respect to plaquing efficiency at 32 and 37°C and plaque size, demonstrating that the nt 1 to 763 region of Db-2 is similar to that of the wild type. The nt 1 to 763 *Pvu*II fragment from the infectious clone was also substituted into the plasmid clone of Db-2. Two individually isolated constructs (Fig. 4, mr5a and mr5b) were tested by DNA transfection, and as expected if the alteration responsible for the Db-2 phenotype resides at nt 946 (Fig. 4B), these constructs performed like cloned Db-2 with respect to both plaque frequency and size. The above results indicate that the mutation responsible for the Db-2 phenotype must lie exclusively within the NS-1 coding region between nts 763 and 1030. Finally, the nt 763 to 1030 region of the Db-2 plasmid was sequenced, and the only alteration from the wild-type sequence was the expected 3-nucleotide insertion at the *Dde*I site at nt 946 (data not shown).

Defective genome amplification in Db. To further characterize the block to viral replication observed for the Db-2 mutant, we examined genome replication during infection over 48 h (enough time for approximately two rounds of infection by wild-type virus) at 32 and 39°C. Parallel cultures of A9 cells highly synchronized at the G1-S boundary by a combination isoleucine deprivation-aphidicolin protocol were infected at each temperature with either wild-type MVM (Fig. 5A) or Db-2 (Fig. 5B) at a multiplicity of infection of 0.3, 10 h before release of the cells from aphidicolin and entrance into the S phase. Viral RFs were monitored by Southern analysis of Hirt extracts from infected cells.

At 16 h p.i., more 5.1-kb double-stranded monomer RF (mRF) DNA was produced by wild-type MVM (Fig. 5A, lanes 4 and 5) than by Db-2 (Fig. 5B, lanes 4 and 5) at both 32 and 39°C. Considerably more mRF DNA was produced by wild-type MVM at 39°C than at 32°C. By 24 h p.i., the amount of wild-type mRF had reached the maximum assayable level at both temperatures (Fig. 5A, lanes 6 and 7). In contrast, the amount of viral RF generated by Db-2 at 16 h p.i. (Fig. 5B, lanes 4 and 5) at 32 and 39°C was approximately equal. By 24 h, the accumulation of Db-2 mRF at 32°C had increased dramatically (Fig. 5B, lanes 6 and 8), whereas the Db-2 mRF accumulated at 39°C did not markedly increase after 16 h p.i. (Fig. 5B, lane 10). These experiments demonstrate that Db-2 is deficient in genome replication and that

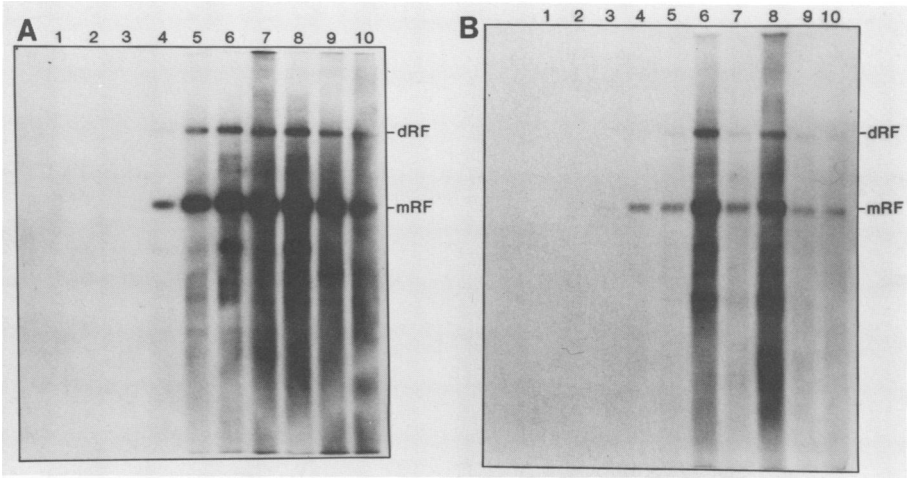

FIG. 5. Db-2 is deficient in genome amplification. Shown are Southern analyses of Hirt extracts taken at various times from highly synchronized A9 cells infected in parallel at 32 and 39°C by wild-type MVM (A) or Db-2 (B) as described in the text. Lanes: 1, at the time of release from aphidicolin (10 h after infection with virions) at 32°C; 2 and 3, 8 h p.i. at 32 and 39°C, respectively; 4 and 5, 16 h p.i. at 32 and 39°C, respectively; 6 and 7, 24 h p.i. at 32 and 39°C, respectively; 8 and 9, 36 h p.i. at 32 and 39°C, respectively; 10, 48 h p.i. at 39°C.

this deficiency is much more pronounced at 39°C. We could not detect an abnormal accumulation of a particular RF (i.e., the 10-kb double-stranded dimer RF [dRF]) in these assays. A more precise analysis of the Db-2 replicative DNA conformers during a single viral burst cycle in highly synchronized cells is in progress.

Deficiency of Db-2 in regulation of temporal order of expression from the two viral promoters independent of the number of accumulated viral templates. The two transcription units of MVM are transcribed in a temporal order; in a highly synchronized MVM(p) infection the transcripts from the P4 promoter (R1 and R2), which produce the nonstructural proteins (16), can be detected before those from the P39 promoter (R3) (13), which become predominant at later times during infection (39). Also, the nonstructural proteins of both the autonomous and nonautonomous parvoviruses have been shown to enhance expression from viral capsid gene promoters in transient cotransfection assays (27, 40, 52). These observations suggest that the parvovirus nonstructural proteins play a role mediating the regulation of viral transcription during lytic infection. We therefore decided to characterize the temporal order of appearance of mRNAs produced by Db-2 at 32 and 39°C. Because Db-2 is deficient in the replication of viral DNA, we monitored the temporal appearance of Db-2 mRNA in relation to the concurrent amplification of viral DNA.

The temporal expression of wild-type MVM and Db mRNAs was assayed by analysis of RNase-protected hybrids formed in solution between excess complementary SP6 promoter-generated MVM RNA probes and total RNA isolated at various times from highly synchronized A9 cells infected at a multiplicity of infection of 0.3 (Fig. 6A and B). Virions were added to cells 10 h before the release of the cells from the aphidicolin block and entrance into the S phase. The MVM *Hae*III D fragment (nts 1854 to 2378) was cloned into the pGEM vector (Promega) and was the template for an RNA probe extending from before the acceptor site of the large splice in R2 mRNA to within the small intron common to all the viral mRNAs at nts 2280 to 2399. The probe fragments which are protected by spliced or unspliced viral R1, R2, and R3 can readily be distinguished on sequencing gels (13). mRNA species employing either of the alternative splice donor sites can be distinguished, but this probe will not distinguish species employing alternative small splice acceptor sites nor differentiate between unspliced R1 RNA and viral DNA. Hirt extractions were done concurrently, and DNA was assayed by Southern analysis to measure genome amplification (Fig. 6a and b).

In the experiment shown in Fig. 6, wild-type MVM R3 mRNAs became the predominant RNA species 6 h after release of infected cells into the S phase at 39°C (Fig. 6A, lane 2). At 32°C, the amounts of wild-type R3 mRNAs were slightly greater than those of R1 and R2 mRNAs at 12 h (Fig. 6A, lane 5), and by 21 h, the R3 transcripts became predominant (Fig. 6A, lane 7). In contrast, during Db-2 infection, the shift to the predominant appearance of the R3 mRNAs was delayed at both 32 and 39°C. At 21 h after release into the S phase, at both 32 and 39°C, the Db-2 R1 and R2 mRNAs were still the predominant species present (Fig. 6B, lanes 1 and 2). By 46 h postrelease, the R3 transcripts became predominant at 32°C (Fig. 6B, lane 3); however, at 39°C, R1 and R2 were still the predominant species present (Fig. 6B, lane 4). (Although the amount of protected probe in Fig. 6B, lane 4, is low, the ratio of P4 to P39 products is still evident.)

Concurrent analysis of Db-2 replicative DNA forms demonstrated that the delay in the shift of the predominance of R3 transcripts in Db-2 infection is not merely the result of less mRF and dRF DNA available for transcription. At 39°C, the R3 mRNAs were the predominant species 6 h after release of the wild-type infections into the S phase (Fig. 6A, lane 2), yet the amount of wild-type viral mRF present (Fig. 6a, lane 2) was considerably less than in the Db-2 infection at 39°C 21 h after release into the S phase (Fig. 6b, lane 2), at which point Db-2 R1 and R2 mRNAs still predominated (Fig. 6B, lane 2). Likewise, at 32°C, 12 h after release of the wild-type infection into the S phase, the R3 mRNAs became the predominant species (Fig. 6A, lane 5), yet the amount of wild-type mRF (Fig. 6a, lane 7) was markedly less than the amount of Db-2 mRF accumulated at 21 h at 32°C (Fig. 6b, lane 1), at which point the Db-2 R1 and R2 mRNAs were still the predominant species (Fig. 6B, lane 1). Therefore, Db-2 R1 and R2 transcripts predominate even when the amounts of Db-2 mRF and dRF exceed the amounts of RFs present in wild-type infection at the time wild-type R3 becomes the predominant transcript. These results suggest that Db-2 is deficient in the regulation of the temporal expression of viral

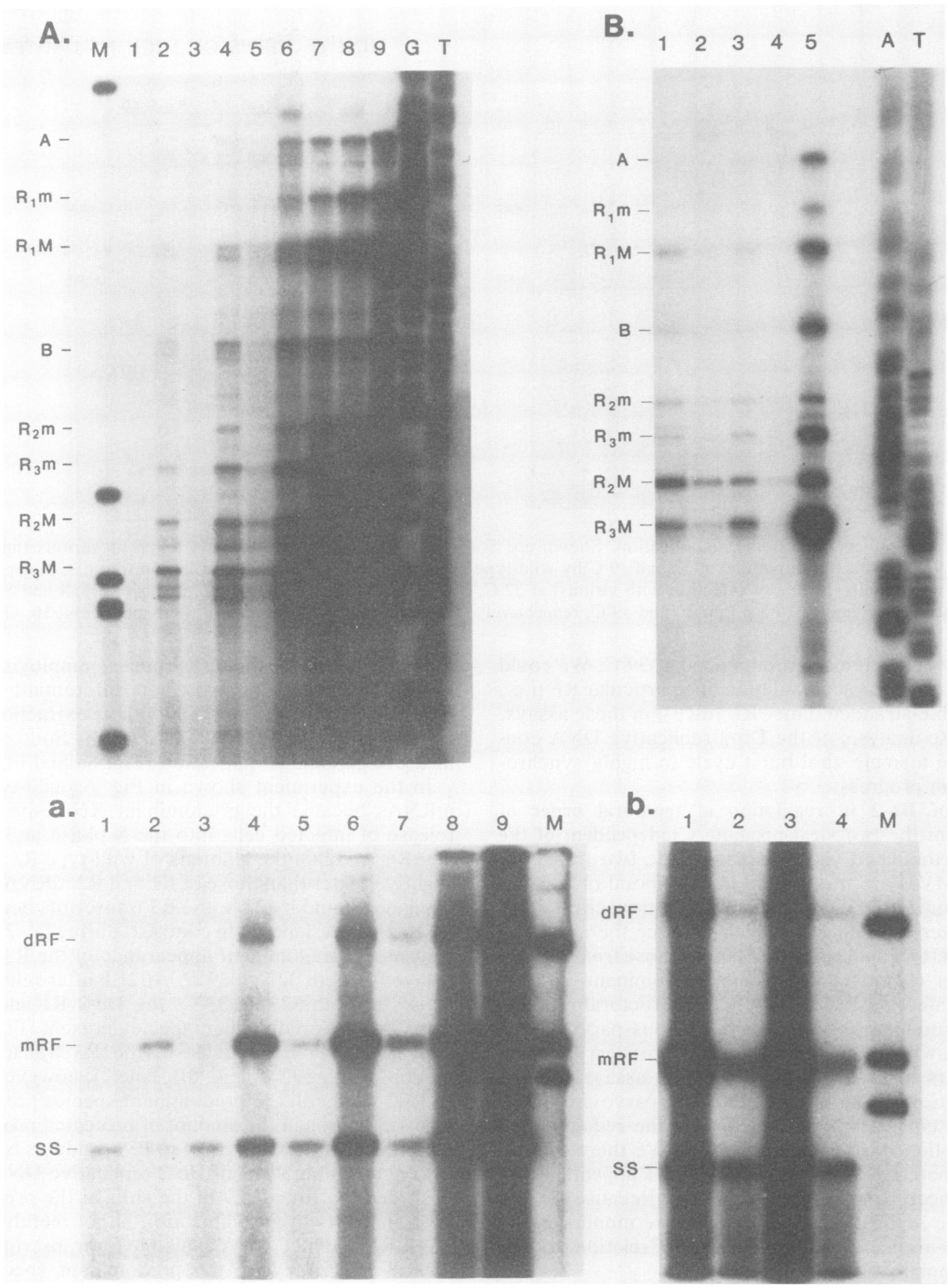

FIG. 6. Db-2 is deficient in regulation of the temporal appearance of transcripts from the two viral promoters independent of the number of accumulated templates. Parallel cultures of highly synchronized A9 cells infected at 32 and 39°C with either wild-type MVM (A and a) or Db-2 (B and b) were assayed for the temporal appearance of transcripts (A and B) by RNase protection assays of 5 μg of total RNA with excess probe, as described in the text and reference 13, or for viral replicative DNA forms (a and b) by Southern analysis of Hirt extracts as described in Materials and Methods. (A) Lanes: M, kinased ϕX174 *Hae*III markers, 603, 310, 281, 271 (doublet), and 234 nt in length; 1, 3, 5, and 7, protected fragments from 32°C wild-type infection at 6, 8, 12, and 21 h, respectively; 2, 4, 6, and 8, protected fragments from 39°C wild-type infection at 6, 8, 12, and 21 h, respectively; 9, protected fragments taken late in infection by wild-type MVM at 37°C; G and T, sequencing tracts with ddGTP and ddTTP, respectively. The gel was overexposed to highlight the bands at the earlier time points. Lighter exposure of lanes 6 to 9 shows a predominance of R3 mRNA characteristic of steady-state mRNA late in viral infection (13) (data not shown). (B) Lanes: 1 and 3, protected fragments from Db-2 infection at 32°C at 21 and 46 h, respectively; 2 and 4, protected fragments from Db-2 infection at 39°C at 21 and 46 h, respectively; 5, same as panel A, lane 9; A and T, sequencing tracts with ddATP and ddTTP, respectively. R1M (426 nt), R1m (463 nt), R2M (290 nt), R2m (327 nt), R3M (275 nt), and R3m (312 nt) are the probe fragments protected by the major (M) and minor (m) spliced MVM R1, R2, and R3 mRNAs; bands A (524 nt) and B (373 nt) represent unspliced R1 and R3, respectively, as described in the text and in reference 13. (a) Lanes: 1, 3, 5, 7, and 9, DNA RFs from 32°C wild-type infections at 6, 8, 10, 12, and 21 h, respectively; 2, 4, 6, and 8, DNA RFs from 39°C wild-type infections at 6, 8, 10, and 12 h, respectively; M, nonradioactive plasmid DNA markers of 9.5, 5.1, and 4.4 kb. (b) Lanes: 1 and 3, DNA RFs from 32°C Db-2 infections at 21 and 46 h, respectively; 2 and 4, DNA RFs from 39°C Db-2 infections at 21 and 46 h, respectively; M, same as panel a, lane M. SS, Single-stranded DNA; mRF, monomer RF; dRF, dimer RF. For Southern analysis, identical amounts of the nonradioactive markers were run on each gel to control for equivalent transfer and the filters were subsequently hybridized with identical amounts of the same nick-translated probe.

mRNAs and that NS-1 is required for this function, independent of its role in viral DNA replication.

DISCUSSION

In-phase amino acid insertion mutations were constructed in the ORF of the NS-1 and NS-2 genes of MVM. Five viable mutants were isolated, two of which appeared to have a wild-type phenotype in DNA transfection plaque assays. The remaining three had defective phenotypes and may be useful in defining the role of NS-1 in the lytic cycle of MVM. One of these mutants, Db-2, in which an isoleucine is inserted in NS-1 between residues 229 and 230, is particularly interesting in that it produces small plaques at 32°C and is almost 3 orders of magnitude more temperature sensitive in plaque-forming ability at 39°C.

Southern analysis of viral RFs demonstrated that Db-2 is deficient in DNA replication at both 32 and 39°C. However, the result is most dramatic at the higher temperature. The relative ratios of mRF and dRF produced during Db-2 infection seem similar to those formed in wild-type samples; therefore, Db-2 does not appear to be defective in the production of a specific RF. We have not as yet distinguished between different conformers of mRF and dRF. We are currently investigating whether Db-2 is deficient in the production of a specific replicative intermediate.

Analysis of the expression of cotransfected plasmids has demonstrated that parvovirus nonstructural proteins transactivate viral capsid gene promoters (27, 40, 52). The availability of an NS-1 mutation enabled us to assay whether this protein plays a role in the regulation of the temporal appearance of viral transcripts during lytic infection. In highly synchronized infection at both 32 and 39°C, Db-2 R1 and R2 transcripts predominated even when the amounts of Db-2 mRF and dRF exceeded the amounts of RFs present in wild-type infection at the time wild-type R3 becomes the predominant transcript. These results suggest that MVM NS-1 is required for the regulation of the temporal expression of viral R3 transcripts independent of its role in DNA replication. However, as noted above, we did not rule out the possibility that Db-2 is deficient in the production of a specific mRF or dRF conformer that is responsible for enhanced transcription of R3.

The isoleucine insertion between residues 229 and 230 in Db-2 is not within regions previously identified as conserved within parvovirus NS-1 genes (4, 44) and which are homologous to ATPase and nucleotide-binding domains of the simian virus 40 and polyomavirus large-T antigens and the papillomavirus E1 proteins (4, 17). However analysis of this insertion in computer-generated protein structure predictions (19, 24) does predict the disruption of a short turn motif between residues 232 and 235 of NS-1. Interestingly, an insertion of a tyrosine just two residues downstream (Hc), which is predicted to extend this turn an extra amino acid, results in a lethal phenotype. We are currently characterizing the thermolability of the Db NS-1 protein by immunoprecipitation after various pulse-chase regimens at both 32 and 39°C.

The nonviable mutants were not characterized further because verification that they contain only the expected insertion mutation is required. However, one of these mutants, Df, was pursued because its location at nt 2277 makes its nonviable phenotype particularly interesting. The *Dde*I site at 2277 encompasses the termination codon of NS-1 (ORF 3), and a correct 3-base insertion at this site would duplicate the TAA termination codon in ORF 3. A 102-nt fragment spanning the altered *Dde*I site in Df was shown by marker exchange experiments similar to those described for Db-2 to be responsible for the Df nonviable phenotype (G. Tullis and D. Pintel, unpublished data). Sequencing of this segment revealed, however, that the Df mutation contains a 2-base insertion between nts 2279 and 2280 rather than the expected 3-base insertion (G. Tullis and D. Pintel, unpublished data). This mutation leaves the termination codon for NS-1 (nucleotides 2276 to 2278) unaltered. The reading frame for NS-2 should be shifted into ORF 1 just before the splice donor site at 2280. Df therefore encodes a different set of carboxyl termini for NS-2. We are currently characterizing this mutant to determine whether it defines a required function for the MVM NS-2 protein during the viral life cycle.

ACKNOWLEDGMENTS

We thank Lisa Burger for excellent technical assistance and Rob Schoborg, Deborah Roussell, and Ram Guntaka for discussion and critique of the manuscript. D.J.P. dedicates this work to the memory of Giampiero di Mayorca.

This work was supported by Public Health Service grants AI-21302 and T32 AI-07276 from the National Institutes of Health and by the Life and Health Insurance Medical Research Fund.

LITERATURE CITED

1. **Arraj, J. A., and M. G. Marinus.** 1983. Phenotypic reversal in *dam* mutants of *Escherichia coli* K12 by a recombinant plasmid containing the *dam*$^+$ gene. J. Bacteriol. **153**:562–565.
2. **Astell, C. R., M. B. Chow, and D. C. Ward.** 1985. Sequence analysis of the termini of virion and replicative forms of minute virus of mice DNA suggests a modified rolling hairpin model for autonomous parvovirus DNA replication. J. Virol. **54**:171–177.
3. **Astell, C. R., E. M. Gardiner, and P. Tattersall.** 1986. DNA sequence of the lymphotropic variant of minute virus of mice, MVM(i), and comparison with the DNA sequence of the fibrotropic prototype strain. J. Virol. **57**:656–669.
4. **Astell, C. R., C. D. Mol, and W. F. Anderson.** 1987. Structural and functional homology of parvovirus and papovavirus polypeptides. J. Gen. Virol. **68**:885–893.
5. **Astell, C. R., M. Thomson, M. B. Chow, and D. C. Ward.** 1983. Structure and replication of minute virus of mice DNA. Cold Spring Harbor Symp. Quant. Biol. **47**:751–762.
6. **Astell, C. R., M. Thomson, M. Merchlinsky, and D. C. Ward.** 1983. The complete DNA sequence of minute virus of mice, an autonomous parvovirus. Nucleic Acids Res. **11**:999–1018.
7. **Barany, F.** 1985. Two-codon insertion mutagenesis of plasmid genes by using single-stranded hexameric oligonucleotides. Proc. Natl. Acad. Sci. USA **82**:4202–4206.
8. **Ben-Asher, E., and Y. Aloni.** 1984. Transcription of minute virus of mice, an autonomous parvovirus, may be regulated by attenuation. J. Virol. **52**:226–276.
9. **Berns, K. I., and M. A. Labow.** 1987. Parvovirus gene regulation. J. Gen. Virol. **68**:601–614.
10. **Bernstein, M. D., N. Sonenberg, and D. Baltimore.** 1985. Poliovirus mutant that does not selectively inhibit host cell protein synthesis. Mol. Cell. Biol. **5**:2913–2923.
11. **Boissy, R., and C. R. Astell.** 1985. An *Escherichia coli recBCsbcBrecF* host permits the deletion-resistant propagation of plasmid clones containing the 5′ terminal palindrome of minute virus of mice. Gene **35**:179–185.
12. **Clemens, K. E., and D. Pintel.** 1987. Minute virus of mice (MVM) mRNAs predominately polyadenylate at a single site. Virology **160**:511–514.
13. **Clemens, K. E., and D. J. Pintel.** 1988. The two transcription units of the autonomous parvovirus minute virus of mice are transcribed in a temporal order. J. Virol. **62**:1448–1451.
14. **Cotmore, S. F., V. C. McKie, L. J. Anderson, C. R. Astell, and P. Tattersall.** 1986. Identification of the major structural and non-structural protein encoded by human parvovirus B19 and

mapping of their genes by procaryotic expression of isolated genomic fragments. J. Virol. **60**:548–557.
15. **Cotmore, S. F., L. J. Sturzenbecker, and P. Tattersall.** 1983. The autonomous parvovirus MVM encodes two non-structural proteins in addition to its capsid polypeptides. Virology **129**:333–343.
16. **Cotmore, S., and P. Tattersall.** 1986. Organization of nonstructural genes of the autonomous parvovirus minute virus of mice. J. Virol. **58**:724–732.
17. **Cotmore, S. F., and P. Tattersall.** 1987. The autonomously replicating parvoviruses of vertebrates. Adv. Virus Res. **33**:91–174.
18. **Cotmore, S. F., and P. Tattersall.** 1988. The NS-1 polypeptide of minute virus of mice is covalently attached to the 5′ termini of duplex replicative-form DNA and progeny single strands. J. Virol. **62**:851–860.
19. **Garnier, J., D. J. Osguthorpe, and B. Robson.** 1978. Analysis of the accuracy and implications of simple methods for predicting the secondary structure of globular proteins. J. Mol. Biol. **120**: 97–120.
20. **Heintz, N. M., J. D. Milbrandt, K. S. Greisen, and J. L. Hamlin.** 1983. Cloning of the initiation region of a mammalian chromosomal replicon. Nature (London) **302**:439–441.
21. **Hermonat, P. L., M. A. Labow, R. Wright, K. I. Berns, and N. Muzyczka.** 1984. Genetics of adeno-associated virus: isolation and preliminary characterization of mutants of adeno-associated type 2 mutants. J. Virol. **51**:611–619.
22. **Hirt, B.** 1967. Selective extraction of polyoma DNA from infected mouse cell cultures. J. Mol. Biol. **26**:363–369.
23. **Jongeneel, C. V., R. Sahli, G. K. McMaster, and B. Hirt.** 1986. A precise map of the splice junctions in the RNAs of the minute virus of mice, an autonomous parvovirus. J. Virol. **59**:564–573.
24. **Kabsch, W., and C. Sander.** 1983. How good are predictions of protein secondary structure? FEBS Lett. **155**:179–182.
25. **Labieniec-Pintel, L., and D. Pintel.** 1986. The minute virus of mice P39 transcription unit can encode both capsid proteins. J. Virol. **57**:1163–1167.
26. **Labow, M. A., L. H. Graf, Jr., and K. I. Berns.** 1987. Adeno-associated virus gene expression inhibits cellular transformation by heterologous genes. Mol. Cell. Biol. **7**:1320–1325.
27. **Labow, M. A., P. L. Hermonat, and K. I. Berns.** 1986. Positive and negative autoregulation of the adeno-associated virus type 2 genome. J. Virol. **60**:251–258.
28. **Lederman, M., S. F. Cotmore, E. R. Stout, and R. C. Bates.** 1987. Detection of bovine parvovirus proteins homologous to the nonstructural NS-1 proteins of other autonomous parvovirus. J. Virol. **61**:3612–3616.
29. **Lederman, M., J. T. Patton, E. R. Stout, and R. C. Bates.** 1984. Virally coded non-capsid protein associated with bovine parvovirus infection. J. Virol. **49**:315–318.
30. **Ley, K. D., and R. A. Tobey.** 1970. Regulation of initiation of DNA synthesis in Chinese hamster cells. J. Cell Biol. **47**:453–459.
31. **Littlefield, J. W.** 1964. Three degrees of guanylic acid-inosinic acid pyrophosphorylase deficiency in mouse fibroblasts. Nature (London) **203**:1142–1144.
32. **Maniatis, T., E. F. Fritsch, and J. Sambrook.** 1982. Molecular cloning, a laboratory manual. Cold Spring Harbor Laboratory, Cold Spring Harbor, N.Y.
33. **Mendelson, E., J. P. Trempe, and B. J. Carter.** 1986. Identification of the *trans*-acting Rep proteins of adeno-associated virus by antibodies to a synthetic oligopeptide. J. Virol. **60**:823–832.
34. **Merchlinsky, M. J., P. Tattersall, J. J. Leary, S. F. Cotmore, E. M. Gardner, and D. C. Ward.** 1983. Construction of an infectious molecular clone of the autonomous parvoviruses minute virus of mice. J. Virol. **47**:227–232.
35. **Morgan, W. R., and D. C. Ward.** 1986. Three splicing patterns are used to excise the small intron common to all minute virus of mice RNAs. J. Virol. **60**:1170–1174.
36. **Ozawa, K., and N. Young.** 1987. Characterization of capsid and noncapsid proteins of B19 parvovirus propagated in human erythroid bone marrow cell cultures. J. Virol. **61**:2627–2630.
37. **Parker, R. C., R. M. Watson, and J. Vinograd.** 1977. Mapping of closed circular DNAs by cleavage with restriction endonucleases and calibration by agarose gel electrophoresis. Proc. Natl. Acad. Sci. USA **74**:851–855.
38. **Pedrali-Noy, G., S. Spadari, A. Miller-Favres, A. O. A. Miller, J. Kruppa, and G. Koch.** 1980. Synchronization of HeLa cell cultures by inhibition of DNA polymerase alpha with aphidicolin. Nucleic Acids Res. **8**:377–387.
39. **Pintel, D., D. Dadachanji, C. R. Astell, and D. C. Ward.** 1983. The genome of minute virus of mice, an autonomous parvovirus, encodes two overlapping transcription units. Nucleic Acids Res. **11**:1019–1038.
40. **Rhode, S. L., III.** 1985. *trans*-Activation of parvovirus p38 promoter by the 76K noncapsid protein. J. Virol. **55**:886–889.
41. **Rhode, S. L., III.** 1987. Construction of a genetic switch for inducible *trans*-activation of gene expression in eucaryotic cells. J. Virol. **61**:1448–1456.
42. **Sanger, F., S. Miklen, and A. R. Coulson.** 1977. DNA sequencing with chain-terminating inhibitors. Proc. Natl. Acad. Sci. USA **74**:5463–5467.
43. **Senapathy, P., J. D. Tratschin, and B. J. Carter.** 1984. Replication of adeno-associated virus DNA: complementation of naturally occurring *rep*$^-$ mutants by a wild-type genome or an *ori*$^-$ mutant and correction of terminal palindrome deletions. J. Mol. Biol. **79**:1–20.
44. **Shade, R. O., M. C. Blundell, S. F. Cotmore, P. Tattersall, and C. R. Astell.** 1986. Nucleotide sequence and genome organization of human parvovirus B19 isolated from the serum of a child during aplastic crisis. J. Virol. **58**:921–936.
45. **Shein, M., and J. F. Enders.** 1962. Multiplication and cytopathogenicity of simian vacuolating virus 40 in cultures of human tissues. Proc. Soc. Exp. Biol. Med. **109**:495–500.
46. **Southern, E. M.** 1975. Detection of specific sequences among DNA fragments separated by gel electrophoresis. J. Mol. Biol. **98**:503–517.
47. **Tattersall, P., and J. Bratton.** 1983. Reciprocal productive and restrictive virus-cell interactions of immunosuppressive and prototype strains of minute virus of mice. J. Virol. **46**:944–955.
48. **Tattersall, P., P. J. Cawte, A. J. Shatkin, and D. C. Ward.** 1976. Three structural polypeptides coded for by minute virus of mice, a parvovirus. J. Virol. **20**:273–289.
49. **Tattersall, P., and D. C. Ward.** 1976. Rolling hairpin model for replication of parvovirus and linear chromosomal DNA. Nature (London) **263**:106–109.
50. **Tattersall, P., and D. C. Ward (ed.).** 1978. Replication of mammalian parvoviruses, p. 3–12. Cold Spring Harbor Laboratory, Cold Spring Harbor, N.Y.
51. **Tratschin, J. D., I. L. Miller, and B. J. Carter.** 1984. Genetic analysis of adeno-associated virus: properties of deletion mutants constructed in vitro and evidence for an adeno-associated virus replication function. J. Virol. **51**:611–619.
52. **Tratschin, J. D., J. Tal, and B. J. Carter.** 1986. Negative and positive regulation in *trans* of gene expression from adeno-associated virus vectors in mammalian cells by a viral rep gene product. Mol. Cell. Biol. **6**:2884–2894.
53. **Trempe, J. P., and B. J. Carter.** 1988. Regulation of adeno-associated virus gene expression in 293 cells: control of mRNA abundance and translation. J. Virol. **62**:68–74.